Ferromagnetic Moment and Spin Rotation Transitions in Tetragonal Antiferromagnetic $Sr_2Cu_3O_4Cl_2$

F. C. Chou,[1] Amnon Aharony,[1,2] R. J. Birgeneau,[1] O. Entin-Wohlman,[2] M. Greven,[1] A. B. Harris,[3]
M. A. Kastner,[1] Y. J. Kim,[1] D. S. Kleinberg,[1] Y. S. Lee,[1] and Q. Zhu[4]

[1]*Center of Materials Science and Engineering, Massachusetts Institute of Technology, Cambridge, Massachusetts 02139*
[2]*School of Physics and Astronomy, Raymond and Beverly Sackler Faculty of Exact Sciences,*
Tel Aviv University, Tel Aviv 69978, Israel
[3]*Department of Physics, University of Pennsylvania, Philadelphia, Pennsylvania 19104*
[4]*Physics Department, Brookhaven National Laboratory, Upton, New York 11973*

$Sr_2Cu_3O_4Cl_2$ is a variant of the lamellar copper oxides, containing an extra Cu^{2+} ion in the center of every second plaquette of the square CuO_2 lattice. The two types of Cu form interpenetrating Heisenberg antiferromagnets, which order at 380 and 40 K. Magnetization measurements yield a small spontaneous ferromagnetic moment below 380 K and two spin rotation transitions. The results are explained in detail by a pseudodipolar coupling between the two Cu lattices. A quantitative analysis of the data yields several previously unknown microscopic coupling constants, relevant to other lamellar, chain, and ladder copper oxides.   [S0031-9007(96)02201-6]

The magnetism of lamellar copper oxides has received much attention, because they both become high temperature superconductors when doped, and are also nearly ideal quantum antiferromagnets [1]. Therefore, these materials provide excellent testing grounds for theories of quantum magnetism. The fundamental building block of materials like La_2CuO_4 is the planar CuO_2 layer consisting of a square lattice with Cu ions on the corners and O ions on the edges. The Cu^{2+} ions represent a $S = 1/2$ square lattice quantum Heisenberg antiferromagnet (SLQHA), with a nearest neighbor (NN) leading isotropic O-mediated superexchange energy $J_0 \approx 130$ meV. These materials have nonzero Néel temperatures due to small interplanar coupling and spin anisotropies [1–3].

Recently, attention has focused on "234" variants of the cuprates, $Sr_2Cu_3O_4Cl_2$ and $Ba_2Cu_3O_4Cl_2$ [4–6]. These materials have an additional Cu ion (denoted by Cu II) at the center of every second plaquette of the CuO_2 lattice (made of Cu I's), creating two interpenetrating square lattices of Cu ions (see Fig. 1) [7]. Similarly to other lamellar cuprates, neutron scattering experiments find Cu I antiferromagnetic (AFM) order below $T_{N,I} \approx 380$ K. In addition, the Cu II's exhibit AFM order below $T_{N,II} \approx 40$ K [4,6,8]. The detailed nature of the Cu II-Cu II and the Cu I-Cu II interactions has not yet been identified. Concerning the former, we provide evidence that, like the Cu I's, the Cu II's represent a SLQHA. The Cu I-Cu II interactions are expected to be quite delicate; since each Cu II is surrounded by four Cu I's, an isotropic Heisenberg interaction would yield frustration, due to a vanishing mean field at the Cu II sites. The present Letter presents information on both the isotropic and the crucial anisotropic terms, as well as on quantum fourfold terms.

The Cu I-O-Cu II and Cu II-O-O-Cu II geometry in 234 is, respectively, the same as that for the NN and next NN (NNN) Cu-Cu pairs in the spin chains which arise, e.g., in $Sr_{14}Cu_{24}O_{41}$ [9]. Our Cu I-O-Cu II geometry is also the same as the interladder one in $Sr_{14}Cu_{24}O_{41}$ and in many ladder cuprates, like $Sr_{n-1}Cu_{n+1}O_{2n}$ [10]. Thus,
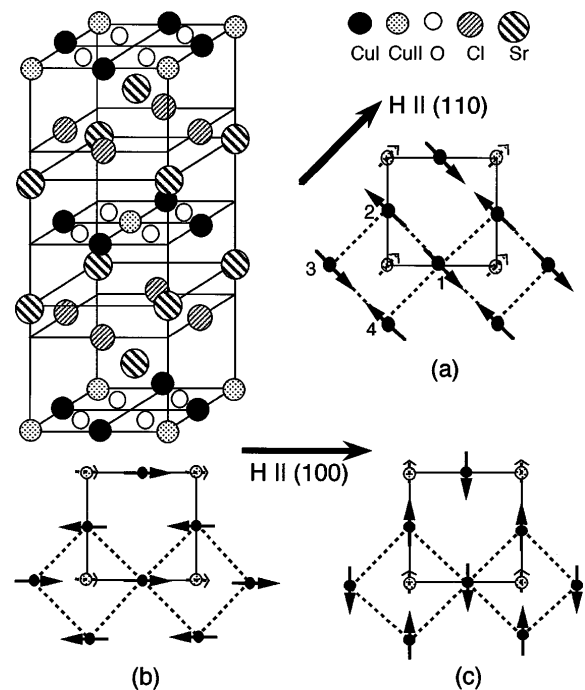
FIG. 1. Structure of $Sr_2Cu_3O_4Cl_2$ and of the Cu_3O_4 layer, including spin configurations for (a) **H** ∥ (110), (b) **H** ∥ (100) and $H_{c1} < H < H_{c2}$, and (c) **H** ∥ (100) and $H_{c2} \ll H$. The figure shows only the part of $\mathbf{M}_{II}$ induced by the internal pseudodipolar field $-4J_{pd}\hat{\Gamma}\mathbf{M}_I^{\dagger}$. A nonzero H induces an additional small canting of the Cu I moments in cases (a) and (c), and a large component of $\mathbf{M}_{II}$ along **H** in case (c) (not shown).

our measured coupling constants in 234 represent estimates for their hitherto unmeasured counterparts in many chain, ladder, and planar cuprates.

Perhaps the most peculiar feature of 234 is a small spontaneous ferromagnetic (FM) moment, $M_S \sim 10^{-3}\mu_B$, which appears at $T_{N,I}$. M_S has been attributed [4–6] to the Dzyaloshinsky-Moriya (DM) antisymmetric exchange. Although this mechanism is effective in orthorhombic La$_2$CuO$_4$ [11], *symmetry forbids it in the perfectly tetragonal structure* of 234: the DM interactions from individual bonds sum up to zero. Thus, the origin of M_S has been a mystery. Here we show that in tetragonal symmetry M_S *must* result from anisotropic pseudodipolar Cu I-Cu II interactions. Similar interactions have been predicted between NN planes in Sr$_2$CuO$_2$Cl$_2$ or Nd$_2$CuO$_4$ [12], but have not yet been measured. We report measurements of the field dependence of the magnetization of Sr$_2$Cu$_3$O$_4$Cl$_2$, $M(H)$, for different directions of the field **H**, which exhibit a rich behavior [including two spin rotation transitions for **H** $\parallel$ (100)], providing detailed quantitative evidence for this theoretical description.

We have focused on Sr$_2$Cu$_3$O$_4$Cl$_2$, for which it is possible to grow large single crystals by slow cooling from a melt containing CuO as flux. Small crystals, $\sim$6 mm $\times$ 7 mm $\times$ 0.5 mm, with the c axis (normal to the Cu$_3$O$_4$ layer) perpendicular to the large face are used for measurements of $M(H)$ with a quantum design SQUID magnetometer at $H < 5.5$ T. High-resolution synchrotron x-ray powder diffraction measurements show that the crystal remains tetragonal (space group $I4/mmm$) for temperatures $15 < T < 550$ K, with lattice contants $a = 5.457$ Å and $c = 12.52$ Å for $T < 50$ K. (The effects of the lower magnetic symmetry are negligible.)

Our measured $M(H)$ becomes simplest for **H** $\parallel$ (110): the susceptibility $\chi \equiv dM/dH$ is independent of H for all $H > 0.1$ T, and the data in this range are fitted by $M(H) = M_S^{(110)}(T) + \chi^{(110)}(T)H$. For $H < 0.1$ T, the system exhibits interesting domain effects [13]. The spontaneous moment $M_S^{(110)}(T)$ is plotted in Fig. 2. The full line in that figure represents a fit near $T_{N,I}$ to $(T_{N,I} - T)^\beta$, with $\beta =$
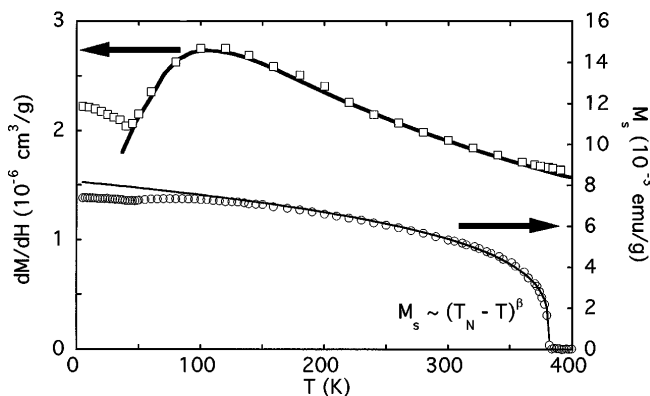
0.27 $\pm$ 0.03 and $T_{N,I} = (382 \pm 2)$ K. β agrees within the errors with those found for the staggered moment $M_I^\dagger$ of the Cu I spins [6,8] and for $M^\dagger$ in Sr$_2$CuO$_2$Cl$_2$ [1] and La$_2$CuO$_4$ [14]. The proportionality $M_S \sim M_I^\dagger$ indicates that the Cu II spins see an effective uniform field proportional to $M_I^\dagger$. Such a field would arise from a bilinear coupling between M_S and $M_I^\dagger$, but this is rather unusual for tetragonal systems.

Figure 2 also shows $\chi^{(110)}(T)$. In principle, $\chi = \chi_{II} + 2\chi_{I,\perp} + \chi_d + \chi_{VV}$, with the diamagnetic core susceptibility $\chi_d \sim -3.3 \times 10^{-7}$ cm^3/g [15], the small contribution of the Cu I's, $2\chi_{I,\perp} \sim 4 \times 10^{-7}$ cm^3/g (see below), and the Van Vleck susceptibility χ_{VV} ($\sim$0.5 $\times$ 10^{-7} cm^3/g, for La$_2$CuO$_4$ [16]). However, fortuitously the last 3 terms add up to zero within the errors, and we have $\chi \approx \chi_{II}$. The solid heavy curve in Fig. 2 represents results for χ_{II} from Monte Carlo simulations of the $S = 1/2$ SLQHA [17], with the single isotropic exchange parameter $J_{II} = (10 \pm 1)$ meV [18]. The detailed quantitative agreement of the simulations with the measured χ_{II} shows that the Cu II system is a new example of a $S = 1/2$ SLQHA. The neutron results confirm this in detail, and take advantage of the small J_{II} to measure the first spin wave spectra of a SLQHA [8]. The actual ordering at $T_{N,II}$ results mainly from an effective Ising anisotropy, caused by the presence of the FM moment on Cu II. Indeed, the neutron experiments for $M_{II}^\dagger$ below 40 K are well fitted with the two dimensional Ising exponent $\beta = 1/8$ [8]. The cusp in χ at 40 K is also typical of an AFM ordering, giving more support for our identification of χ with χ_{II}.

When **H** is not along (110), χ becomes H dependent, and M becomes smaller than its value along (110), implying competing interactions. We thus identify (110) as the *easy axis*. For large H, the staggered moment of the Cu I's becomes perpendicular to **H**, gaining from the larger perpendicular susceptibility $\chi_{I,\perp}$. Therefore, χ approaches the *same* limit $\chi^{(110)}$, for *all* the directions of **H**. To emphasize the deviations from these parallel asymptotes, we plot $m(H, \alpha) = (M - \chi^{(110)}H)/M_S^{(110)}$, when **H** $\equiv H(\cos\alpha, \sin\alpha, 0)$ (Fig. 3). At $T = 200$ K and $\alpha = 0$, χ becomes H independent between two critical fields, $H_{c1} = 0.3$ T and $H_{c2} = 1.7$ T, indicated by arrows in Fig. 3, implying that $M(H) = M_S^b + \chi^b H$, with $\chi^b < \chi^{(110)}$ and $M_S^b < M_S^{(110)}$. χ does vary with H outside of this intermediate region, with discontinuities at H_{c1} and H_{c2}. As we show below, the variation of χ with H reflects a rotation of $\mathbf{M}_I^\dagger$ between the structures shown in Figs. 1(a)–1(c). We observe no such sharp transitions at $\alpha \neq 0$, or at lower T.

We now introduce our theoretical model. Since we ignore the Cu II-Cu II interactions [13], the following results apply only for $T_{N,II} < T < T_{N,I}$. Consider a Cu I-Cu II bond along $\hat{x} \equiv (100)$ (Fig. 1). Since there exist two mirror planes which contain this bond, one perpendicular to the tetragonal z axis and the other containing that axis, the most general form allowed for the symmetric Cu I-Cu II

FIG. 2. Saturated FM moment $M_S^{(110)}$ and susceptibility $\chi^{(110)}$. The full lines represent $M_S \sim (T_{N,I} - T)^\beta$ and a simulation of χ_{II} for the $S = 1/2$ SLQHA (see text).
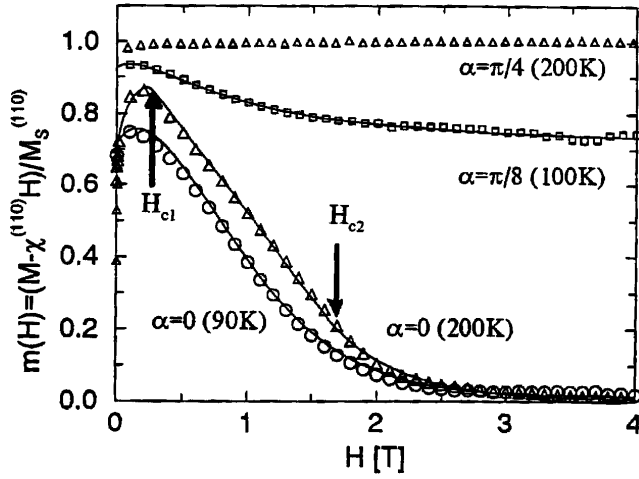
FIG. 3. Theoretical (full lines) and measured values of $m(H, \alpha)$.

interaction must be of the form

$$\mathcal{H}_{I-II} = J^{\|} S_I^{\|} S_{II}^{\|} + J^{\perp} S_I^{\perp} S_{II}^{\perp} + J^z S_I^z S_{II}^z, \quad (1)$$

where $\|$ and $\perp$ denote parallel and perpendicular to the Cu I-Cu II bond [12]. Denoting the 4 Cu I's adjacent to a Cu II by 1, 2, 3, and 4 for the $\hat{x}$, $\hat{y}$, $-\hat{x}$, and $-\hat{y}$ directions, and restricting all the spins to the XY plane (as found experimentally), the sum over these four bonds yields

$$\mathcal{H}_{I-II} = 4\mathbf{M}_{II} \cdot (J_{av}\mathbf{M}_I + J_{pd}\hat{\Gamma}\mathbf{M}_I^{\dagger}), \quad (2)$$

where $2J_{av} = (J^{\|} + J^{\perp})$, $2J_{pd} = (J^{\|} - J^{\perp})$, $\mathbf{M}_{II} = \mathbf{S}_{II}$, while $\mathbf{M}_I = \sum_{I=1}^4 \mathbf{S}_{I,i}/4$ and $\mathbf{M}_I^{\dagger} = (\mathbf{S}_{I,1} - \mathbf{S}_{I,2} + \mathbf{S}_{I,3} - \mathbf{S}_{I,4})/4$ represent the FM and AFM Cu I moments [18]. Here, $\hat{\Gamma} \equiv \sigma_z$ is the 2×2 Pauli matrix: $\hat{\Gamma}(x, y) \equiv (x, -y)$. In addition to the isotropic average J_{av}, J_{pd} represents an *anisotropic* "pseudodipolar" net interaction, which yields a bilinear coupling between $\mathbf{M}_I^{\dagger}$ and $\mathbf{M}_{II}$. As soon as $\mathbf{M}_I^{\dagger}$ orders, it generates a net field $-4J_{pd}\hat{\Gamma}\mathbf{M}_I^{\dagger}$ on the Cu II in the center of each plaquette. Since the Cu II's occupy only every second plaquette, they are all surrounded by exactly the same configuration of Cu I moments (both in each plane and in adjacent planes) [8]. Therefore they all see the *same* local field and have the same FM moment [Figs. 1(a)–1(c)] [19].

If $\mathbf{M}_I^{\dagger} \equiv M_I^{\dagger}(\cos\theta, \sin\theta)$, the second term in Eq. (2) is minimized when $\mathbf{M}_{II} \| \hat{\Gamma}\mathbf{M}_I^{\dagger} = M_I^{\dagger}(\cos\theta, -\sin\theta)$, and the energy of this term is the same for all θ. In particular, the cases $\theta = -\pi/4, 0$ and $-\pi/2$, shown in Figs. 1(a)–1(c), respectively, have the same energy, which is the minimum of this term for $J_{pd} < 0$. However, once $\mathbf{M}_{II} \neq 0$ (due to the second term), the first term generates a small FM moment $\mathbf{M}_I \| \mathbf{M}_{II}$. Since $\chi_{I,\perp} > \chi_{I,\|}$ ($\|$ and $\perp$ to $\mathbf{M}_I^{\dagger}$), such a moment is easier to generate in the configuration of Fig. 1(a), when the Cu I spins can cant so that $\mathbf{M}_I \perp \mathbf{M}_I^{\dagger}$, than in that of Fig. 1(b), which would require $\mathbf{M}_I \| \mathbf{M}_I^{\dagger}$. This yields a fourfold symmetry, which prefers ordering of $\mathbf{M}_{II}$ along (110), as indeed observed experi-

mentally at low H. An additional fourfold anisotropy energy, of the form $\mathcal{H}_4 = K\cos 4\theta$, with $K > 0$, which also prefers ordering along (110), has been shown to arise for the Cu I's in other cuprates, due to quantum fluctuations [12]. (It does not arise as a single ion term for $S = 1/2$.) Indeed, our quantitative fits to the data require adding $\mathcal{H}_4$, with K close to the value predicted in Ref. [12].

The anisotropic interactions in Eq. (1) could result from the usual dipole-dipole interactions. For the NN bonds, this yields $J^{\|} = -2J^{\perp} = -2(g\mu_B)^2/r^3 \approx -20 \mu eV$, where $r = a/2$ is the Cu I-Cu II bond length, so that $J_{pd} < 0$. However, similar anisotropic terms may also arise from direct or superexchange interactions involving spin-orbit and Coulomb exchange interactions, and these sometimes yield $J_{pd} > 0$, implying a flipping of $\mathbf{M}_{II}$ in Fig. 1 [12]. Therefore, we call these terms pseudodipolar. A measurement of the relative directions of the spins would identify the sign of J_{pd}.

Adding $\mathbf{H}$, Eq. (2) becomes $\mathcal{H} = -2\mathbf{H} \cdot \mathbf{M}_I - \mathbf{H}_{II} \cdot \mathbf{M}_{II}$, with $\mathbf{H}_{II} = \mathbf{H} - 4J_{av}\mathbf{M}_I - 4J_{pd}\hat{\Gamma}\mathbf{M}_I^{\dagger}$. (The factor 2 is the number of Cu I's per planar unit cell, which contains one Cu II.) Assuming a linear response of the Cu II's, i.e., $\mathbf{M}_{II} \approx \chi_{II}\mathbf{H}_{II}$, one finds a mean field energy per unit cell $E = E_0(I) - 2\mathbf{H} \cdot \mathbf{M}_I - \chi_{II}(\mathbf{H}_{II})^2/2 + \mathcal{H}_4$, where $E_0(I)$ contains the unperturbed energy of the Cu I's. For $T \ll T_{N,I}$, it is sufficient to use a low temperature approximation, in which $E_0(I) = 4J_0[\mathbf{M}_I^2 - (\mathbf{M}_I^{\dagger})^2]$, $(\mathbf{M}_I)^2 + (\mathbf{M}_I^{\dagger})^2 = (\mathbf{S}_I)^2 \equiv S^2$, and $\mathbf{M}_I \perp \mathbf{M}_I^{\dagger}$, implying that (without quantum corrections) $\chi_{I,\perp}(T) \approx \chi_{I,\perp}(0) = 1/(8J_0)$ and $\chi_{I,\|} = 0$. Neglecting $J_{pd}^2, J_{pd}H$ in comparison with J_{av}^2 and minimizing with respect to M_I gives $E(\theta) = -[\chi_{II} + 2\tilde{\chi}\sin^2(\theta - \alpha)]H^2/2 + M_0 H[\cos(\theta + \alpha) + y\sin 2\theta \sin(\theta - \alpha)] - k\sin^2 2\theta + \text{const}$, where $\tilde{\chi} = (1 - 2J_{av}\chi_{II})^2/[8(J_0 - \chi_{II}J_{av}^2)] \approx \chi_{I,\perp}(0)$, $M_0 = 4J_{pd}\chi_{II}M_I^{\dagger}$, $y = -4J_{av}\tilde{\chi}/(1 - 2J_{av}\chi_{II})$, and $k = 2K + (M_0 y/2)^2/\tilde{\chi}$. Having solved $\partial E/\partial\theta = 0$ for θ, the measured moment is

$$M = -\partial E/\partial H = [\chi_{II} + 2\tilde{\chi}\sin^2(\theta - \alpha)]H$$
$$- M_0[\cos(\theta + \alpha) + y\sin 2\theta \sin(\theta - \alpha)]. \quad (3)$$

Equation (3) reproduces all of our experimental results. For $\alpha = \pi/4$, the minimum occurs at $\theta = \pi/4 + \text{sgn}(J_{pd})\pi/2$, leading to the structure shown in Fig. 1(a) and to $\chi^{(110)} = (\chi_{II} + 2\tilde{\chi})$ and $M_S^{(110)} = |M_0|(1 + y)$. For very large H, the minimum obeys $\theta - \alpha \approx \text{sgn}(J_{pd})\pi/2 - M_S^{(110)}\cos 2\alpha/2\tilde{\chi}H$, and hence $M = \chi^{(110)}H + M_S^{(110)}\sin 2\alpha + \mathcal{O}(1/H)$, consistent with the parallel asymptotes in Fig. 3. In this limit, $\mathbf{M}_I^{\dagger} \perp \mathbf{H}$.

For $\alpha = 0$, the equation $\partial E/\partial\theta = 0$ exhibits special behavior: $\sin\theta = 0$ is *always* an extremum. When the quadratic equation $2\tilde{\chi}H^2 - |M_0|(1 - 4y)H + 8k = 0$ has two real and positive solutions $H_{c1,2}$, then $\sin\theta = 0$ is the only solution for $H_{c1} < H < H_{c2}$. This gives the structure of Fig. 1(b), and the straight $M(H)$ with $\chi^b = \chi_{II}$ and $M_S^b = |M_0|$. For other values of H, the

537

minimum has a nonzero $|\cos\theta|$, which starts at $\sqrt{2}/2$ for $H = 0$ [yielding the structure in Fig. 1(a)], increases towards 1 at $H = H_{c1}$, where it remains up to H_{c2}, corresponding to Fig. 1(b), and decreases towards 0 [i.e., Fig. 1(c)] as H increases towards ∞ above H_{c2}. This reproduces our data at 200 K, and relates them to spin rotations between Figs. 1(a)–1(c). For all $\alpha \neq 0$, and also when the solutions $H_{c1,2}$ do not exist (as happens at lower T), the solution $\sin\theta = 0$ never applies, the sharp transitions disappear, and there is only one continuous solution for θ.

Having extracted $M_S^{(110)}$ and $\chi^{(110)}$ from the data for $\alpha = \pi/4$ (results given in Fig. 2), we next plot $m(H, \alpha)$ for other α's. The function m depends only on $\tilde{\chi}/M_S^{(110)}$, y, and $k/\tilde{\chi}$. All of our data for $70 \leq T \leq 120$ K are consistent with Eq. (3), with the *temperature independent* parameters $\tilde{\chi} = (0.22 \pm 0.01) \times 10^{-6}$ cm^3/g, $y = 0.03 \pm 0.02$, and $K = (10 \pm 3) \times 10^{-7}$ meV (full lines in Fig. 3). The error bars represent ranges of acceptable fits. The agreement with the data is excellent: $m(H, \alpha)$ turns out to be sensitive to α near 0, and our "(100)" data are fit best with $\alpha \approx 0.2°-0.4°$, which is within the alignment error. From y and $\tilde{\chi}$ we extract $J_{\text{av}} \approx -(12 \pm 9)$ meV. Using the quantum renormalization $\chi_{\text{I},\perp} \approx 0.53/8J_0$ [17], $\tilde{\chi}$ gives $J_0 = (130 \pm 40)$ meV, roughly the same as in other cuprates. K is in rough agreement with the predictions of Ref. [12]. It has been too small to be measured directly in other cuprates. Using $M_{\text{I}}^{\dagger} \approx 0.3$ [17], we finally find $|J_{\text{pd}}| = (27 \pm 1)$ μeV, which is of the same order as the dipolar $J_{\text{pd}} \approx -20$ μeV. Our measured isotropic interaction J_{av} is much larger and FM, probably indicating superexchange and direct exchange. The graph for 200 K has somewhat different parameters: $\tilde{\chi} = (0.165 \pm 0.006) \times 10^{-6}$ cm^3/g, $y = 0.008 \pm 0.004$, and $K = (5 \pm 1) \times 10^{-7}$ meV. At higher T, $\chi_{\text{I},\perp}$ should be replaced by $\chi_{\text{I},\perp} - \chi_{\text{I},\parallel}$, a quantity whose decrease to zero as T increases towards $T_{N,\text{I}}$ explains the observed decrease in $\tilde{\chi}$. The T dependence of y and K is not yet understood. Unlike the parameters used at low T, the parameters at 200 K yield spin rotation transitions and reproduce the experimentally observed H_{c1} and H_{c2}.

In addition to providing convincing evidence that the pseudodipolar interaction is the source of the ferromagnetism in 234, our experiments yield quantitative measurements of the previously unknown parameters K, J_{II}, J_{av}, and J_{pd}. Results below $T_{N,\text{II}}$ also confirm our theory [13]. It would be interesting to compare our values of J_{av} and J_{pd} with the Cu-Cu interladder coupling (J_{av} has been predicted to be FM there [10], but is thought to be AFM for the NN interaction in the chain system [9]). Since the isotropic interladder coupling is also frustrated, we expect it to be dominated by our J_{pd}. It would also be interesting to understand the relevance of J_{II} to the NNN Cu-Cu coupling in other lamellar cuprates and to study the consequences of our values of J_{av}, J_{pd}, and J_{II} for the NN and NNN interactions in the chains. Our results imply a large NNN/NN ratio which could explain the mysterious gap observed there [9]. The sign of J_{pd} should determine if the chain spins prefer ordering parallel or perpendicular to the chains.

[1] M. Greven, R. J. Birgeneau, Y. Endoh, M. A. Kastner, M. Matsuda, and G. Shirane, Z. Phys. B **96**, 465 (1995).

[2] B. Keimer, A. Aharony, A. Auerbach, R. J. Birgeneau, A. Cassanho, Y. Endoh, R. W. Erwin, M. A. Kastner, and G. Shirane, Phys. Rev. B **45**, 7430 (1992).

[3] B. Keimer, N. Belk, R. J. Birgeneau, A. Cassanho, C. Y. Chen, M. Greven, M. A. Kastner, A. Aharony, Y. Endoh, R. W. Erwin, and G. Shirane, Phys. Rev. B **46**, 14 034 (1992).

[4] S. Noro, T. Kouchi, H. Harada, T. Yamadaya, M. Tadokoro, and H. Suzuki, Mater. Sci. Eng. B **25**, 167 (1994).

[5] H. Ohta, M. Sumikawa, M. Motokawa, S. Noro, and T. Yamadaya, J. Phys. Soc. Jpn. **64**, 1759 (1995).

[6] K. Yamada, N. Suzuki, and J. Akimitsu, Physica (Amsterdam) **213&214B**, 191 (1995).

[7] B. Grande and H. Müller-Buschbaum, Z. Naturforsch. **31B**, 405 (1976).

[8] M. Greven *et al.* (unpublished).

[9] M. Matsuda and K. Katsumata, Phys. Rev. B **53**, 12 201 (1996).

[10] E. Dagotto and T. M. Rice, Science **271**, 618 (1996).

[11] T. Thio, T. R. Thurston, N. W. Preyer, P. J. Picone, M. A. Kastner, H. P. Jenssen, D. R. Gabbe, C. Y. Chen, R. J. Birgeneau, and A. Aharony, Phys. Rev. B **38**, 905 (1988).

[12] T. Yildirim, A. B. Harris, A. Aharony, and O. Entin-Wohlman, Phys. Rev. B **52**, 10 239 (1995).

[13] F. C. Chou *et al.* (unpublished).

[14] T. Thio and A. Aharony, Phys. Rev. Lett. **73**, 894 (1994).

[15] P. Selwood, *Magnetochemistry* (Interscience, New York, 1956), p. 78.

[16] D. C. Johnston, Phys. Rev. Lett. **62**, 957 (1989).

[17] M. Makivic and H.-Q. Ding, Phys. Rev. B **43**, 3562 (1991); M. Greven, Ph.D. thesis, M.I.T., 1995.

[18] In the theory we use dimensionless moments S, M, and measure the various J's, H, and $1/\chi$ in ergs. To translate into the experimental units of emu/g and cm^3/g, multiply M by $g\mu_B/m_{uc} = 22.4$ emu/g, where $g = 2$ and $m_{uc} = 500$ g/$N_A = 83 \times 10^{-23}$ g, and χ by $(g\mu_B)^2/m_{uc} = 4.16 \times 10^{-19}$ erg cm^3/g. Using $g = 2.2$ will modify some of the parameters slightly.

[19] In fact, a low T state with finite $\mathbf{M}_{\text{I}} \parallel \mathbf{M}_{\text{II}} \perp \mathbf{M}_{\text{I}}^{\dagger}$ would be generated by J_{av} alone even when $J_{\text{pd}} = 0$. However, this requires $J_{\text{av}}^2 \chi_{\text{II}} > J_0$, which is not obeyed here. [E. F. Shender, Sov. Phys. JETP **56**, 178 (1982); J. Stein, A. Aharony, O. Entin-Wohlman, and A. B. Harris (unpublished)].